ACS OMEGA

http://pubs.acs.org/journal/acsodf

Article

Naphthalene Endoperoxide Heterodimer Designed for Sustained Singlet Oxygen Release

Ziang Liu, Hao Wu, Jin Li, Lei Wang,* and Engin U. Akkaya*

Cite This: *ACS Omega* 2021, 6, 26799−26804

Read Online

ACCESS | Metrics & More | Article Recommendations | Supporting Information

ABSTRACT: Naphthalene endoperoxides undergo thermal cycloreversion reactions to produce singlet oxygen and their parent naphthalene compounds. The rate of the reaction is dependent on the structural features, such as steric and electronic modulators. We believe that achieving a sustained release rate of singlet oxygen is important in potential biological applications. This can be achieved by tethering of two endoperoxides with different singlet oxygen release rates in a single molecular construct. Here, we report the synthesis of such a dimeric endoperoxide. Our data shows that with the biexponential reaction kinetics of singlet oxygen generation from a heterodimeric endoperoxide, it is possible to hold singlet oxygen release rates within a selected range for a longer period of time.

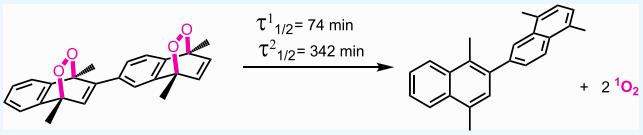

INTRODUCTION

Singlet oxygen is one of the reactive oxygen species (ROS) known to be involved in a number of biological processes as a signaling entity[1,2] and also in the photodynamic therapy of cancers and other lesions.[3,4] While it can be generated photochemically by the process of photosensitization,[5−10] its chemical generation under mild conditions is attracting recent attention.[11−13] Singlet oxygen is highly reactive and, as a consequence, has a very short half-life and diffusion distance in aqueous solutions[14] and more so in biological media.[15]

Biological production of singlet oxygen takes place in a number of processes, such as oxidative phosphorylation, photosynthesis, and the action of myeloperoxidase.[16,17] It is also possible to generate this particular ROS by the reactions of phosphine/phosphite ozonides,[18] molybdate,[19] chloramine, or HOCl with H_2O_2.[20,21] However, these chemical reactions proceed under very harsh oxidative conditions, which are not amenable to fine control. Among the milder chemical sources of singlet oxygen, endoperoxides of naphthalene,[22] anthracene,[23] and 2-pyridone[24] have attracted the most attention. Previous works have shown that by changing substituents or the substitution pattern, it is possible to obtain endoperoxides of widely differing singlet oxygen release (cycloreversion) rates and yields.[23,24]

Most chemical processes in living systems are far from equilibrium. Considering the potential biological utility of chemically produced singlet oxygen, it appears that the rate of singlet oxygen release may be more important than the total amount of singlet oxygen release. In fact, the recent literature suggests that for the singlet oxygen production rate, there seems to be a threshold rate of reactivity[25] and also an upper limit, above which harmful effects may dominate. Singlet oxygen generated at a lower rate would be chemically effectively quenched by GSH.[26]

Extended release of singlet oxygen based on a rational design will be of great importance. In this study, we designed a dimeric endoperoxide **9**, which not only releases more singlet oxygen but also holds the release rates within a selected range for a longer time (Figure 1).

RESULTS AND DISCUSSION

One way to achieve a longer sustained level of singlet oxygen release may be incorporating multiple singlet oxygen sources with different reactivities in one chemical structure. We previously found that 1,4-naphthalene endoperoxide with a substitution at the 2-position showed slower singlet oxygen release. With these considerations, we chose to synthesize the target compound **9** (Figure 2). To confirm the advantages gained by this approach, two monomeric endoperoxides **4** and **7** were synthesized as models for the two tethered naphthalene cores in the form of a 2,6′-dimer. The synthesis plan for these endoperoxides is straightforward. Briefly, 2-bromo-1,4-dimethylnaphthalene **2** was obtained by the dark bromination of the precursor compound **1** (Figure 2). During the reaction, light exposure should be avoided, as it may lead to undesired radical halogenation of the methyl groups. Product **2** can be easily separated from the reaction mixture in excellent yield. Suzuki coupling with the commercially available phenylboronic acid in a toluene/ethanol/water solvent mixture yields compound **3** in good yields. The model endoperoxide for 2-aryl substitution **4**

Received: August 19, 2021
Accepted: September 24, 2021
Published: October 4, 2021

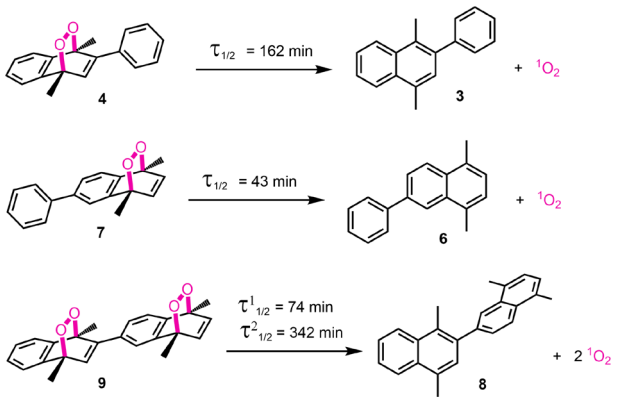

Figure 1. Dimeric endoperoxide **9** and model compounds **4** and **7**, shown together with the experimentally determined half-life values in this work. The reactions were carried out at 37 °C.

was obtained by irradiating a $CDCl_3$ solution with a red LED array at 630 nm under an oxygen atmosphere. The synthesis for the model endoperoxide for 6-aryl substitution **7** makes use of a very useful regioselective borylation at the 6-position reported by Suginome's group.[27] Using this method, the borylated compound **5** was obtained at very high yields (up to 98%). Direct coupling of this compound with iodobenzene gives 6-phenyl-substituted naphthalene **6**, which can be converted to the corresponding endoperoxide **7** under standard photosensitized oxygenation conditions (*vide supra*). Finally, the 2,6′-endoperoxide heterodimer **9** was obtained by the Suzuki coupling of compounds **2** and **5**, followed by the reaction with the photogenerated singlet oxygen. Hydrolytic removal of the pinacol functionality in ester in **5** followed by Suzuki coupling results in losses of yield. So, the direct reaction of the ester is preferable. The cycloreversion reactions of compounds **4**, **7**, and **9** were followed by ^{1}H NMR measurement as the characteristic peaks (Figure 3) can easily be identified. Considering that the singlet oxygen release follows a first-order reaction kinetics, the half-life of endoperoxide can be calculated according to the half-life formula ($\tau_{1/2} = \ln 2/k$). The temporal evolutions of the NMR spectra (Supporting Information) were relatively simple for compounds **4** and **7** and yielded first-order decay rate constants, which give the half-life values for these compounds (**4**: $\tau_{1/2}$ = 2.7 h; **7**: $\tau_{1/2}$ = 0.71 h; see the Supporting Information). Values are in accordance with the expectations based on larger steric hindrance by the 2-aryl substituent, resulting in a lower release rate of singlet oxygen. The dimeric endoperoxide yields somewhat complicated NMR data because of the changes in the peaks resulting from two reactions with different rates. Fortunately, it is possible to identify two sets of peaks to base rate calculations (Figure 3). The singlet at 1.69 ppm is a characteristic methyl peak for the faster converting naphthalene core, as well as the peaks at 7.08−7.15 ppm. For the slower converting naphthalene core, the peaks emerging at 7.95 ppm are useful. The half-times for the two naphthalene endoperoxide units are thus determined to be 1.23 and 5.7 h.

To confirm singlet oxygen production, we carried out an experiment with the model compounds **4** and **7** and the dimer **9** with the singlet oxygen probe diphenylisobenzofuran (DPBF). As shown in Figure 4, the significant reduction of the characteristic absorbance peak of DPBF at 417 nm was observed after the incubation with corresponding endoperoxides. Among monomeric endoperoxides **4** and **7**, 6-substituted endoperoxide **7** showed a faster release of singlet oxygen, which is in accord with our expectations.

Once the rates of the two distinct cycloreversion reactions of the dimer were determined, it was possible to calculate the total rate of the singlet oxygen production as a function of time and compare it to the individual endoperoxide units in compound **9**. In that comparison, we assume two times larger concentrations for mono-endoperoxide units compared to the dimer **9**. The total rate (from both endoperoxide sources) for the dimer is normalized. The plots of the singlet oxygen generation reaction rates for the compound **9** (1× concentration) and the 6-substituted and 2-substituted naphthalene units (2× concentration) are very revealing. In the shorter time range (Figure 5, 0−4 h), the dimer as a whole releases singlet oxygen faster than the 2-substituted unit but slower than the 6-substituted unit. After 4 h, the release rate of singlet oxygen for the 6-substituted unit decreases very fast (Figure 6). So, for the first 10 h time range, the dimer releases singlet oxygen in a particular rate,

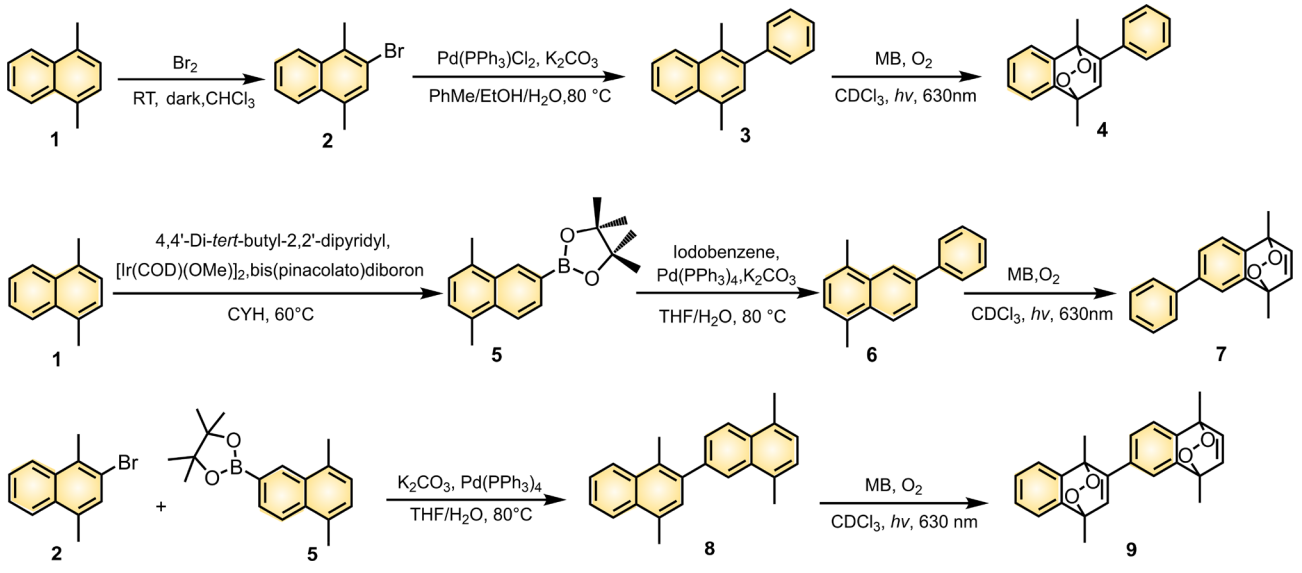

Figure 2. Synthesis of compounds **4**, **7**, and **9**.

https://doi.org/10.1021/acsomega.1c04518
ACS Omega 2021, 6, 26799−26804

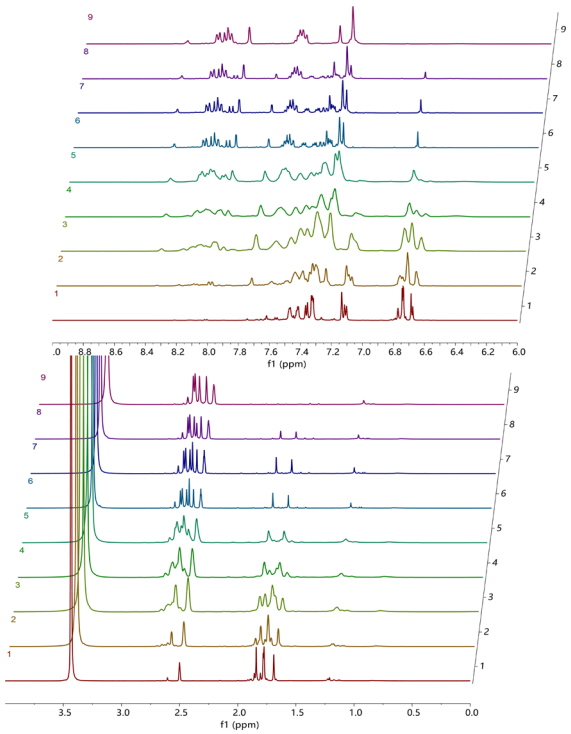

Figure 3. Time evolution of the ^{1}H NMR spectra of compound **9** incubated in DMSO-d_6 at 37 °C. Spectra 1: 0 h; 2: 0.5 h; 3: 1.5 h; 4: 3 h; 5: 5 h; 6: 7 h; 7: 9 h; 8: 11 h; 9: 24 h. Top: low field; bottom: high field.

between 0.7 and 0.05 units, and thus may sustain effective singlet oxygen release for a longer period of time. (Calculations of the data for Figures 5 and 6 are available in the Supporting Information.)

CONCLUSIONS

In conclusion, we were able to synthesize a dimeric endoperoxide, which thermally releases 20% of its mass, as singlet oxygen. The design of the compound allows a biexponential singlet oxygen release due to different levels of steric modulation on the cycloreversion reaction rate. The result is a compound that can sustain a predetermined level of singlet oxygen release rate for a longer time. A simple mixture of the endoperoxides cannot guarantee a similar result because of the potential differences in localization, *in vivo* or *in cellulo*. In consideration of potential biological applications, we expect this approach to generate interest. Our own work toward a library of organic singlet oxygen sources of various reactivities is in progress.

EXPERIMENTAL SECTION

General Information. All reagents and solvents were purchased from commercial suppliers and used without further purification. Reactions were monitored by thin-layer chromatography using Merck TLC silica gel 60 F-254. Column chromatography was performed by using Merck silica gel 60 (particle size: 200−300 mesh). The ^{1}H and ^{13}C NMR spectra were recorded using a Varian DLG400 NMR spectrometer. Chemical shifts are reported in parts per million (ppm), and coupling constants (J values) are given in Hz. Splitting patterns are indicated as follows: s, singlet; d, doublet; t, triplet; m, multiplet. The UV−Vis absorption spectra were obtained by using an Agilent Cary-3500 UV−Vis spectrophotometer. The

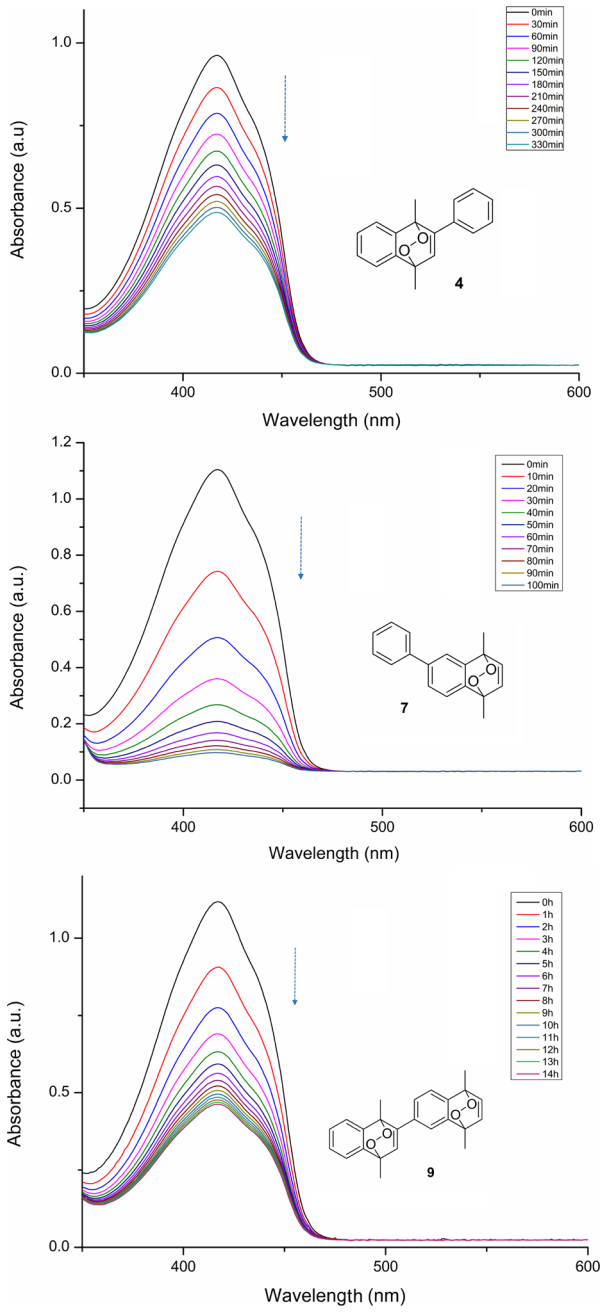

Figure 4. Decreasing absorption at 417 nm of the singlet oxygen trap DPBF (40 μM) at 417 nm with time in DMSO in response to the addition of endoperoxides **4**, **7**, and **9** (200 μM) at 37 °C in the dark, respectively.

mass spectra were recorded with a Thermo Scientific LTQ Orbitrap XL.

Synthesis. *Synthesis of* ***2***. 1,4-Dimethylnaphthalene (1.56 g, 10.0 mmol) was dissolved in 15.0 mL of chloroform under argon and exclusion of light. Bromine (0.54 mL, 10.5 mmol) was added to the reaction mixture over 10 min at 0 °C. The reaction mixture was stirred at room temperature for 4 h and monitored by TLC. Then, the reaction mixture was diluted with 50.0 mL of chloroform and washed with 50.0 mL of saturated $Na_2S_2O_3$ solution, 50.0 mL of water, and 50.0 mL of brine. The organic layer was combined and dried over anhydrous Na_2SO_4. The solution was filtered through a thin pad of silica gel. After the removal of the solvent by a rotary evaporator, the crude product

https://doi.org/10.1021/acsomega.1c04518
ACS Omega 2021, 6, 26799−26804

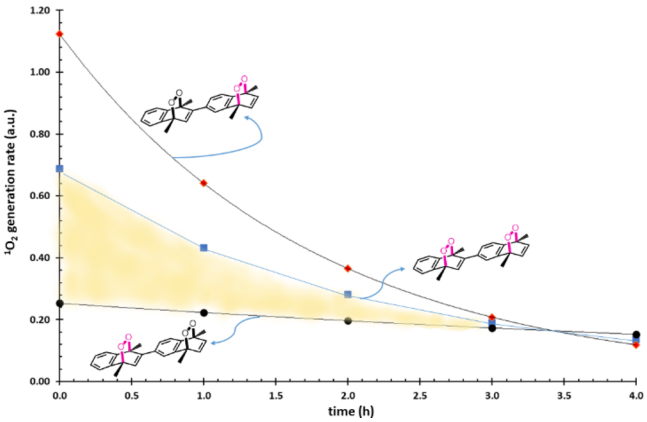

Figure 5. Singlet oxygen generation rate (arbitrary units) as a function of time for the dimer **9** (blue squares) and for the 6-substituted (red diamonds) and 2-substituted units (black circles) (multiplied by 2 to account for the two endoperoxides in one heterodimeric structure). Expanded view of 0−4 h.

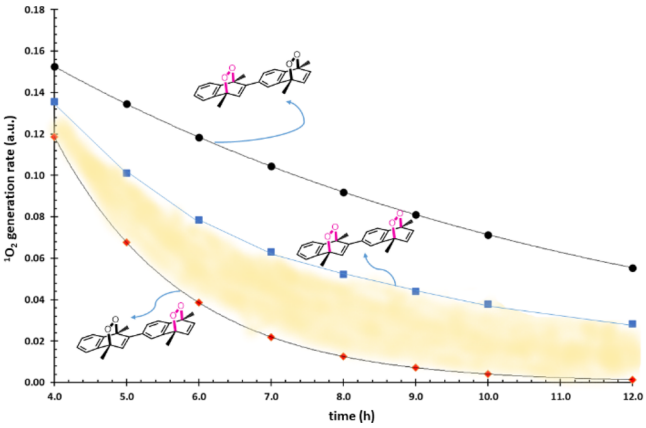

Figure 6. Singlet oxygen generation rate (arbitrary units) as a function of time for the dimer **9** (blue squares) and for the 6-substituted (red diamonds) and 2-substituted units (black circles) (multiplied by 2 to account for the two endoperoxides in one dimeric structure). Expanded view of 4−12 h.

was purified by silica gel column chromatography with hexane as the eluent. The product was obtained in 95% yield (2.22 g). ^{1}H NMR (400 MHz, $CDCl_3$) δ 8.05−8.02 (m, 1H), 7.96−7.94 (m, 1H), 7.55−7.51 (m, 2H), 7.47 (s, 1H), 2.76 (s, 3H), 2.62 (s, 3H); ^{13}C NMR (100 MHz, $CDCl_3$) δ 134.0, 133.5, 131.8, 131.3, 130.5, 126.4, 125.6, 125.0, 124.8, 122.3, 19.0, 18.7.

Synthesis of ***3***. Compound **2** (800 mg, 3.418 mmol), phenylboronic acid (584 mg, 4.786 mmol), and K_2CO_3 (756 mg, 2 mmol) were dissolved in a solution of toluene (6 mL), ethanol (3 mL), and water (3 mL). $Pd(PPh_3)Cl_2$ (120 mg, 0.1709 mmol) was added to the solution before degassing the mixture via bubbling nitrogen. The resulting mixture was stirred at 80 °C under Ar for 8 h. After the reaction was completed, the mixture was diluted with DCM, washed with H_2O, and dried over Na_2SO_4. The solvent was removed under reduced pressure, and the residue was purified by column chromatography with hexane as the eluent. The product was obtained in 76% yield (601 mg). MS-EI m/z calcd for $C_{18}H_{16}$: 232.3; found: 232.0. ^{1}H NMR (400 MHz, $CDCl_3$) δ 8.20−8.18 (m, 1H), 8.12−8.09 (m, 1H), 7.67−7.59 (m, 2H), 7.53−7.49 (m, 2H), 7.45−7.41 (m, 3H), 7.33 (s, 1H), 2.76 (s, 3H), 2.65 (s, 3H); ^{13}C NMR (100 MHz, $CDCl_3$) δ 142.9, 138.8, 133.2, 132.0, 131.8, 129.8, 129.1, 128.9, 128.1, 126.7, 125.9, 125.3, 125.2, 124.6, 19.3, 16.2.

Synthesis of ***4***. Compound **3** (30 mg, 0.129 mmol) was dissolved in 3 mL of $CDCl_3$ at 0 ° C. A catalytic amount of methylene blue was added into the solution, and the mixture was stirred under an oxygen atmosphere with irradiation via 630 nm red light. After the reaction was completed, the solvent was removed by a rotary evaporator, and the crude product was purified by silica gel column chromatography with DCM as the eluent. The product was obtained in 98% yield (33.41 mg). ^{1}H NMR (400 MHz, $CDCl_3$) δ 7.40−7.31 (m, 7H), 7.23−7.20 (m, 2H), 6.55 (s, 1H), 1.96 (s, 3H), 1.78 (s, 3H).

Synthesis of ***5***. A mixture of $[Ir(COD)(OMe)]_2$ (0.165 g, 0.25 mmol), 4,4′-di-*tert*-butyl-2,2′-dipyridyl (0.134 g, 0.5 mmol), bis(pinacolato)diboron (1.395 g, 5.5 mmol), and 1,4-dimethylnaphthalene (0.77 mL, 5 mmol) in cyclohexane (19 mL) was heated at 60 °C for 20 h. After cooling to room temperature, the solvent was removed *in vacuo*. The crude product was purified by a silica gel column with hexane:EtOAc (20:1, v/v). The product was obtained in 81% yield (1.142 g). ^{1}H NMR (400 MHz, $CDCl_3$) δ 8.43 (s, 1H), 7.86 (d, J = 8.4 Hz, 1H), 7.79 (d, J = 8.4 Hz, 1H), 7.11−7.05 (m, 2H), 2.61 (s, 3H), 2.52 (s, 3H), 1.27 (s, 12H); ^{13}C NMR (100 MHz, $CDCl_3$) δ 133.3, 132.3, 131.7, 131.1, 131.0, 129.1, 126.4, 125.1, 122.7, 82.8, 23.9, 18.5, 18.3.

Synthesis of ***6***. Compound **5** (800 mg, 2.84 mmol), iodobenzene (445 mg, 2.18 mmol), and K_2CO_3 (602.59 mg, 2 mmol) were dissolved in THF (20 mL) and water (6 mL). $Pd(PPh_3)_4$ (141 mg, 0.12 mmol) was added to the solution under nitrogen for 30 min. The resulting mixture was stirred at 80 °C for 8 h. After the reaction was completed, the mixture was diluted with DCM, washed with H_2O, and dried over Na_2SO_4. The solvent was removed under reduced pressure, and the residue was purified by column chromatography with hexane as the eluent. The product was obtained in 82% yield (541 mg). MS-EI m/z calcd for $C_{18}H_{16}$: 232.3; found: 232.0. ^{1}H NMR (400 MHz, $CDCl_3$) δ 8.27 (d, J = 1.9 Hz, 1H), 8.15 (d, J = 8.7 Hz, 1H), 7.87−7.84 (m, 1H), 7.83−7.81 (m, 2H), 7.59−7.55 (m, 2H), 7.48−7.44 (m, 1H), 7.32−7.27 (m, 2H), 2.79 (s, 3H), 2.76 (s, 3H); ^{13}C NMR (100 MHz, $CDCl_3$) δ 141.6, 138.1, 133.0, 132.6, 132.3, 131.9, 128.9, 127.6, 127.3, 126.8, 126.4, 125.3, 125.0, 122.8, 19.5, 19.4.

Synthesis of ***7***. Compound **6** (30 mg, 0.129 mmol) was dissolved in 3 mL of $CDCl_3$. The reaction mixture was cooled to 0 °C in an ice bath. A catalytic amount of methylene blue was added into the solution, and the mixture was stirred under an oxygen atmosphere with irradiation via 630 nm red light. After the reaction was completed, the solvent was removed by a rotary evaporator, and the crude product was purified by silica gel column chromatography with DCM as the eluent. The product **7** was obtained in 99% yield (33.76 mg). ^{1}H NMR (400 MHz, $CDCl_3$) δ 7.60−7.58 (m, 2H), 7.54 (d, J = 1.7 Hz, 1H), 7.51−7.46 (m, 3H), 7.42−7.37 (m, 2H), 6.75 (s, 2H), 1.97 (s, 3H), 1.95 (s, 3H).

Synthesis of ***8***. Compound **2** (300 mg, 1.063 mmol), compound **5** (275 mg, 1.169 mmol), and K_2CO_3 (295 mg, 2.216 mmol) were dissolved in THF (20 mL) and water (6 mL). $Pd(PPh_3)_4$ (70 mg, 0.06 mmol) was added to the solution before degassing the mixture via bubbling nitrogen for 30 min. The resulting mixture was stirred under an Ar atmosphere at 80 °C for 5 h. After the reaction was completed, the mixture was diluted with DCM, washed with H_2O, and dried over Na_2SO_4. The solvent was removed under reduced pressure and the

https://doi.org/10.1021/acsomega.1c04518
ACS Omega 2021, 6, 26799−26804

residue was purified by column chromatography with hexane as the eluent. The product was obtained in 84% yield (277 mg). MS-EI m/z calcd for $C_{18}H_{16}$: 310.4; found: 310.0. ^{1}H NMR (400 MHz, $CDCl_3$) δ 8.09−8.07 (m, 1H), 8.02−7.99 (m, 2H), 7.93 (d, J = 1.2 Hz, 1H), 7.55−7.48 (m, 3H), 7.29 (s, 1H), 7.19 (s, 3H), 2.66−2.65 (m, 6H), 2.60 (s, 3H), 2.56 (s, 3H); ^{13}C NMR (100 MHz, $CDCl_3$) δ 138.7, 137.9, 132.1, 131.5, 131.4, 131.3, 131.0, 130.8, 130.4, 128.2, 128.1, 126.6, 125.7, 125.2, 124.9, 124.3, 124.1, 123.6, 123.3, 18.41, 18.36, 18.33, 15.3.

Synthesis of ***9***. Compound **8** (30 mg, 0.129 mmol) was dissolved in 3 mL of $CDCl_3$. The reaction mixture was cooled to 0 °C in an ice bath. A catalytic amount of methylene blue was added into the solution, and the mixture was stirred under an oxygen atmosphere with irradiation via 630 nm red light. After the reaction was completed, the solvent was removed by a rotary evaporator, and the crude product was purified by silica gel column chromatography with DCM as the eluent. The product **9** was obtained in 97% yield (46.85 mg). ^{1}H NMR (400 MHz, DMSO-d_6) δ 7.54−7.47 (m, 2H), 7.43−7.42 (m, 1H), 7.39−7.38 (m, 2H), 7.20 (s, 1H), 7.18−7.17 (m, 1H), 6.81−6.78 (m, 2H), 6.75−6.74 (m, 1H), 1.90 (s, 3H), 1.84 (m, 6H), 1.75 (s, 3H).

■ ASSOCIATED CONTENT

Supporting Information

The Supporting Information is available free of charge at https://pubs.acs.org/doi/10.1021/acsomega.1c04518.

Additional spectral data, MS, and time evolution of the ^{1}H NMR spectra (PDF)

■ AUTHOR INFORMATION

Corresponding Authors

Lei Wang − *State Key Laboratory of Fine Chemicals and Department of Pharmaceutical Sciences, Dalian University of Technology, Dalian 116024, China*; Email: leiwang@dlut.edu.cn

Engin U. Akkaya − *State Key Laboratory of Fine Chemicals and Department of Pharmaceutical Sciences, Dalian University of Technology, Dalian 116024, China*; orcid.org/0000-0003-4720-7554; Email: eua@dlut.edu.cn

Authors

Ziang Liu − *State Key Laboratory of Fine Chemicals and Department of Pharmaceutical Sciences, Dalian University of Technology, Dalian 116024, China*

Hao Wu − *State Key Laboratory of Fine Chemicals and Department of Pharmaceutical Sciences, Dalian University of Technology, Dalian 116024, China*

Jin Li − *State Key Laboratory of Fine Chemicals and Department of Pharmaceutical Sciences, Dalian University of Technology, Dalian 116024, China*

Complete contact information is available at: https://pubs.acs.org/10.1021/acsomega.1c04518

Notes

The authors declare no competing financial interest.

■ ACKNOWLEDGMENTS

The authors gratefully acknowledge support from LiaoNing Revitalization Talents Program (E.U.A.: XLYC1902001; L.W.: XLYC1907021) and the National Science Foundation of China (L.W.: 22007008).

■ REFERENCES

(1) Dogra, V.; Kim, C. Singlet Oxygen Metabolism: From Genesis to Signaling. *Front. Plant Sci.* **2020**, *10*, 1640.

(2) Kochevar, I. E. Singlet oxygen signaling: From intimate to global. *Sci. STKE* **2004**, pe7.

(3) Niedre, M. J.; Yu, C. S.; Patterson, M. S.; Wilson, B. C. Singlet oxygen luminescence as an in vivo photodynamic therapy dose metric: validation in normal mouse skin with topical amino-levulinic acid. *Br. J. Cancer* **2005**, *92*, 298−304.

(4) Yamamoto, J.; Yamamoto, S.; Hirano, T.; Li, S.; Koide, M.; Kohno, E.; Okada, M.; Inenaga, C.; Tokuyama, T.; Yokota, N.; Terakawa, S.; Namba, H. Monitoring of singlet oxygen is useful for predicting the photodynamic effects in the treatment for experimental glioma. *Clin. Cancer Res.* **2006**, *12*, 7132−7139.

(5) Kwon, N.; Kim, H.; Li, X.; Yoon, J. Supramolecular agents for combination of photodynamic therapy and other treatments. *Chem. Sci.* **2021**, *12*, 7248−7268.

(6) Turksoy, A.; Yildiz, D.; Akkaya, E. U. Photosensitization and controlled photosensitization with BODIPY dyes. *Coord. Chem. Rev.* **2019**, *379*, 47−64.

(7) Yesilgul, N.; Uyar, T. B.; Seven, O.; Akkaya, E. U. Singlet Oxygen Generation with Chemical Excitation of an Erythrosine−Luminol Conjugate. *ACS Omega* **2017**, *2*, 1367−1371.

(8) Lan, M.; Zhao, S.; Liu, W.; Lee, C.-S.; Zhang, W.; Wang, P. Photosensitizers for Photodynamic Therapy. *Adv. Healthcare Mater.* **2019**, *8*, 1900132.

(9) Li, X.; Lee, S.; Yoon, J. Supramolecular photosensitizers rejuvenate photodynamic therapy. *Chem. Soc. Rev.* **2018**, *47*, 1174−1188.

(10) Ogilby, P. R. Singlet oxygen: there is indeed something new under the sun. *Chem. Soc. Rev.* **2010**, *39*, 3181−3209.

(11) Ucar, E.; Xi, D.; Seven, O.; Kaya, C.; Peng, X.; Sun, W.; Akkaya, E. U. "Off−on" switching of intracellular singlet oxygen release under biocompatible conditions. *Chem. Commun.* **2019**, *55*, 13808−13811.

(12) Ayan, S.; Gunaydin, G.; Yesilgul-Mehmetcik, N.; Gedik, M. E.; Seven, O.; Akkaya, E. U. Proof-of-principle for two-stage photodynamic therapy: hypoxia triggered release of singlet oxygen. *Chem. Commun.* **2020**, *56*, 14793−14796.

(13) Fudickar, W.; Linker, T. Release of Singlet Oxygen from Organic Peroxides under Mild Conditions. *ChemPhotoChem* **2018**, *2*, 548−558.

(14) Breitenbach, T.; Kuimova, M. K.; Gbur, P.; Hatz, S.; Schack, N. B.; Pedersen, B. W.; Lambert, J. D. C.; Poulsen, L.; Ogilby, P. R. Photosensitized production of singlet oxygen: Spatially-resolved optical studies in single cells. *Photochem. Photobiol. Sci.* **2009**, *8*, 442−452.

(15) Kuimova, M. K.; Yahioglu, G.; Ogilby, P. R. Singlet oxygen in a cell: spatially dependent lifetimes and quenching rate constants. *J. Am. Chem. Soc.* **2009**, *131*, 332−340.

(16) Steinbeck, M. J.; Khan, A. U.; Karnovsky, M. J. Intracellular singlet oxygen generation by phagocytosing neutrophils in response to particles coated with a chemical trap. *J. Biol. Chem.* **1992**, *267*, 13425−13433.

(17) Winterbourn, C. C.; Kettle, A. J. Redox reactions and microbial killing in the neutrophil phagosome. *Antioxid. Redox Signaling* **2013**, *18*, 642−660.

(18) Bartlett, P. D.; Mendenhall, G. D.; Durham, D. L. Controlled generation of singlet oxygen at low temperatures from triphenyl phosphite ozonide. *J. Org. Chem.* **1980**, *45*, 4269−4271.

(19) Boehme, K.; Brauer, H. D. Generation of singlet oxygen from hydrogen peroxide disproportionation catalyzed by molybdate ions. *Inorg. Chem.* **1992**, *31*, 3468−3471.

(20) Greer, A. Christopher Foote's Discovery of the Role of Singlet Oxygen [$^1O_2$ ($^1\Delta_g$)] in Photosensitized Oxidation Reactions. *Acc. Chem. Res.* **2006**, *39*, 797−804.

(21) Evans, D. F.; Upton, M. W. Studies on singlet oxygen in aqueous solution. Part 1. Formation of singlet oxygen from hydrogen peroxide with two-electron oxidants. *J. Chem. Soc., Dalton Trans.* **1985**, 1141−1145.

(22) Klapper, M.; Linker, T. New singlet oxygen donors based on naphthalenes: Synthesis, physical chemical data, and improved stability. *Chem. − Eur. J.* **2015**, *21*, 8569−8577.

(23) Aubry, J.-M.; Pierlot, C.; Rigaudy, J.; Schmidt, R. Reversible Binding of Oxygen to Aromatic Compounds. *Acc. Chem. Res.* **2003**, *36*, 668−675.
(24) Matsumoto, M.; Yamada, M.; Watanabe, N. Reversible 1,4-cycloaddition of singlet oxygen to N-substituted 2-pyridones: 1,4-endoperoxide as a versatile chemical source of singlet oxygen. *Chem. Commun.* **2005**, 483−485.
(25) Zhu, T. C.; Kim, M. M.; Liang, X.; Finlay, J. C.; Busch, T. M. In-vivo singlet oxygen threshold doses for PDT. *Photonics Lasers Med.* **2015**, *4*, 59−71.
(26) Devasagayam, T. P. A.; Sundquist, A. R.; Di Mascio, P.; Kaiser, S.; Sies, H. Activity of thiols as singlet molecular oxygen quenchers. *J. Photochem. Photobiol., B* **1991**, *9*, 105−116.
(27) Yamamoto, T.; Ishibashi, A.; Koyanagi, M.; Ihara, H.; Eichenauer, N.; Suginome, M. C−H Activation-Based Transformation of Naphthalenes to 3-Iodo-2-naphthylboronic Acid Derivatives for Use in Iterative Coupling Synthesis of Helical Oligo(naphthalene-2,3-diyl)s. *Bull. Chem. Soc. Jpn.* **2017**, *90*, 604−606.

https://doi.org/10.1021/acsomega.1c04518
ACS Omega 2021, 6, 26799−26804